DEVELOPING FINITE ELEMENT MODEL OF THE FRICTION STIR WELDING FOR TEMPERATURE CALCULATION

Iurii GOLUBEV, Anton NAUMOV, Vesselin MICHAILOV

St. Petersburg State Polytechnical University, St. Petersburg, Russian Federation

Abstract

The purpose of this research was development of the model for temperature field analysis under friction stir welding. Mathematical asymmetric heat source model was studied, its capability in comparison with experimental results was proved. Two-dimensional temperature field distribution was studied using Ansys software. Necessary experimental results were obtained by means of welding experiment where the 400x125x2 mm plates were welded. The temperature was measured using thermocouples. Aluminum alloy EN AW 6082 T6 was chosen as a material for workpieces. The simulation model is tasted with experimental result. The results of the simulation are in good agreement with experimental results. Influence of clamps and back plate during friction stir welding was found.

Keywords: Friction stir welding, aluminum alloy, numerical simulation.

1. INTRODUCTION

The use of lightweight materials in aviation, automobile industry and mechanical engineering is of great technical and economic interest. At the same time material strength and welded joints reliability requirements are growing.

In order to meet these requirements, new methods of welding are applied. One of such methods is the friction stir welding. The method is based on the penetration of the rotary tool, so-called pin, into the material of the joined plates. As a result of friction between tool and workpiece the material is heated to temperature close to the melting point. Unlike joints obtained by traditional welding methods this new process has an advantage of obtaining of continuous joint without melt. Such joints have the higher fatigue strength.

Surely, there are factors influencing the properties of the produced joint during new welding process. First of all, this is temperature change as a result of friction. It is a defining factor of forming of mechanical and plastic properties of material and the final properties of the joint in a whole.

High accuracy of temperature determination is possible by using thermocouples. Temperature determination in the zone of plastic deformation and nugget using this method is difficult. Numerical simulation enables an additional ability of temperature determination including in zone of plastic deformation and nugget.

The purpose of this research was to develop the model for temperature field analysis under friction stir welding.

2. EXPERIMENTAL SETUP

This experiment dealt with a welded joints butt weld of two identical plates with the following dimensions: thickness of 2 mm, width of 125 mm and length 400 mm. Aluminum alloy EN AW 6082 T6 was chosen as a material for workpieces. The chemical composition, mechanical and thermo-physical properties of workpiece material are presented in **Tables 1 - 5**, respectively.

Table 1 Chemical composition (wt.%) [1]

Si	Fe	Cu	Mn	Mg	Cr	Zn	Ti	Al
0.7-1.3	0.5	0.1	0.4-1.0	0.6-1.2	0.25	0.2	0.1	Rest.

Table 2 Mechanical properties [1]

R_m (MPa)	$R_{p0.2}$ (MPa)	A_{50} (%)	*HB*	ρ (kg/dm^3)
275-300	240-255	6-9	84-91	2.7

Table 3 Thermal conductivity

T (°C)	20	100	200	300	400	500	600	700
λ (W/m·K)	0.17	0.175	0.18	0.185	0.189	0.192	0.1945	0.195

Table 4 Specific enthalpy

T (°C)	20	100	200	340	400	450	595	1300
H (J/mm^3)	0	0.2343	0.5059	0.9135	1.113	1.2834	1.922	3.605

Table 5 Convection coefficient

T (°C)	20	100	200	300	400	500	600	700	800
h_f (·10^{-5} W/mm^2·K)	2.5	2.722	3.143	3.729	4.508	5.511	6.765	8.3	10.41

The tool used in this study was made of tool steel, having shoulder diameter of 12.5 mm. The pin height was 1.8 mm, its diameter was 4 mm. Plates were placed on backing plate made of alloy steel X20CrMo17 1 and pressed using clamps made of unalloyed steel S355. Weld length from the point of plunging to the point of the tool retracting from the plates was 360 mm. FSW parameters used in this study are listed in **Table 6**.

Table 6 FSW work parameters

Rotation speed (rpm)	Welding speed (mm/min)	Pressure force (kN)	Depth of plunge (mm)	Angle of slope of tool shoulder
710	400	5	1.9	2°

The temperature was measured using thermocouples with the next rigging, **Table 7**.

Table 7 Rigging for the temperature measuring

Type of the thermocouples	Type K
Amplifier	Quantum X
Frequency	5 Hz

In order to have the entire picture of the temperature field in friction stir welding, it was necessary to measure the temperature across the thickness and width of the workpiece. Experimental temperature distribution of the plate was calculated by using thermocouple. Location of the thermocouples is shown in **Fig. 1**.

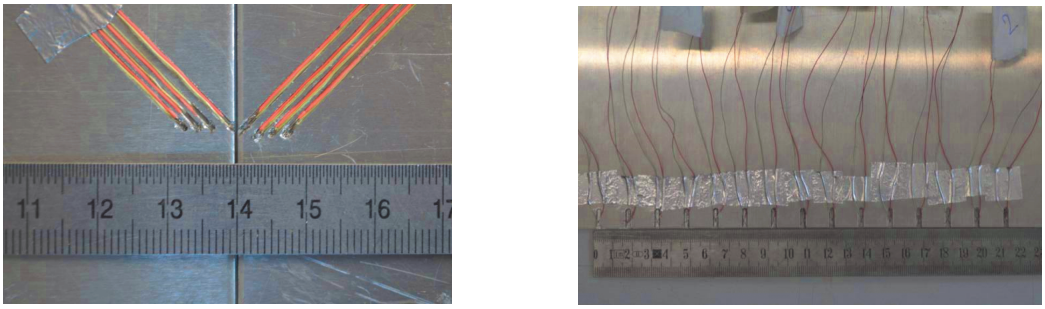

Fig. 1 Location of the thermocouples during temperature measurement across the thickness (to the right) and across the width of the workpieces (to the left)

Measurements were taken on advancing side and retreating side of workpiece to confirm the hypothesis of asymmetric heat source and the thermal field. The plates were prepared in a special way, as shown in **Fig. 1**. The experimental results are presented at the end of the article.

3. MATHEMATICAL MODEL OF FSW

3.1 Mathematical thermal modeling

The task (problem) of the thermal modeling is to calculate the transient temperature fields developed in the workpiece during friction stir welding. In the thermal analysis, the transient temperature field *T* which is a function of the spatial coordinates (*x, y)* and of time *t,* is estimated by the two dimensional nonlinear heat transfer equation, if the heat source is a fast moving source [2]

$$c_i p_i \frac{\partial T}{\partial t} = \frac{\partial}{\partial x}\left(\lambda_i \frac{\partial T}{\partial x}\right) + \frac{\partial}{\partial y}\left(\lambda_i \frac{\partial T}{\partial y}\right) + q_3 \tag{1}$$

where λ is the coefficient of thermal conductivity, c is the mass-specific heat capacity, ρ is the density of the materials and q_3 is heat power density.

Initial condition

$$T(x, y, 0) = T_{env} \tag{2}$$

Boundary condition

$$T|_{S_1} = T_{env} \tag{3}$$

where S_1 is first-order condition.

$$-\lambda_2 \frac{\partial T}{\partial n}\Big|_{S_{3A}} = \alpha_{Al}(T)(T - T_{env}) \tag{4}$$

where λ_2 is the coefficient of thermal conductivity of the aluminum alloy, S_{3A} is third-order boundary condition.

$$-\lambda_1 \frac{\partial T}{\partial n}\Big|_{S_{3S}} = \alpha_{St}(T)(T - T_{env}) \tag{5}$$

where λ_1 is the coefficient of thermal conductivity of unalloyed steel S355, S_{3S} is third-order boundary condition.

3.2 Heat input generation during FSW

Heating of the workpiece is the result of the friction and plastic deformation. Heat output can be written as

$$q_{gen} = q_{friction} + q_{deformation} \tag{6}$$

Heat output due to friction can be calculated as [3]

$$q_{friction} = \frac{2}{3}\pi\omega\left(\left(R_{shoulder}^3 - R_{pin}^3\right)(1-\tan\alpha) + R_{pin}^2 + 3R_{pin}^2 H_{pin}\right)\left((1-\delta)\mu\sigma + \delta\frac{\sigma_{yield}}{\sqrt{3}}\right) \quad (7)$$

where ω is the angular velocity, $R_{shoulder}$ is shoulder radius, R_{pin} is pin radius, H_{pin} is pin height, μ is the friction coefficient, σ is the contact pressures, σ_{yield} is yield stress, α is angle of slope of tool shoulder and δ is the contact state variable. Heat output due to plastic deformation ranges from 2 to 20 % [4] then

$$q_{gen} = k\frac{2}{3}\pi\omega\left(\left(R_{shoulder}^3 - R_{pin}^3\right)(1-\tan\alpha) + R_{pin}^2 + 3R_{pin}^2 H_{pin}\right)\left((1-\delta)\mu\sigma + \delta\frac{\sigma_{yield}}{\sqrt{3}}\right) \quad (8)$$

where from $k = 0.2$ to 1.2.

Translational motion and asymmetric heat source are ignored in the equation (8). Taking translational motion and asymmetric contact conditions into account, we obtain the following equation for advancing side

$$q_{gen} = k\frac{2}{3}\pi\left(\omega\left(\left(R_{shoulder}^3 - R_{pin}^3\right)(1-\tan\alpha) + R_{pin}^2 + 3R_{pin}^2 H_{pin}\right) + V\right)\left((1-\delta)\mu\sigma + \delta\frac{\sigma_{yield}}{\sqrt{3}}\right) \quad (9)$$

where δ = 0.6 and for retreating side

$$q_{gen} = k\frac{2}{3}\pi\left(\omega\left(\left(R_{shoulder}^3 - R_{pin}^3\right)(1-\tan\alpha) + R_{pin}^2 + 3R_{pin}^2 H_{pin}\right) - V\right)\left((1-\delta)\mu\sigma + \delta\frac{\sigma_{yield}}{\sqrt{3}}\right) \quad (10)$$

where δ = 0.4.

Heat source is taken in the cylinder shape and evenly distributed over the cylinder volume

$$q_3 = \frac{\eta q_{gen}}{V} \quad (11)$$

where η is energy conversion efficiency and V is cylinder volume.

$$V = \pi r_0^2 s \quad (12)$$

where s is plate thickness, r_0 is cylindrical heat source radius and calibrated parameter.

Parameter r_0 initially was equal to the tool shoulder radius, and then its value during calibration was varied.

4. FINITE ELEMENT SIMULATION OF FSW PROCESS

Simulation was performed using Ansys Version 14 software. The geometric cross-sectional model of size 254 mm width and 107 mm height was built, **Fig. 2**. Model was symmetric relatively the *y* - axis.

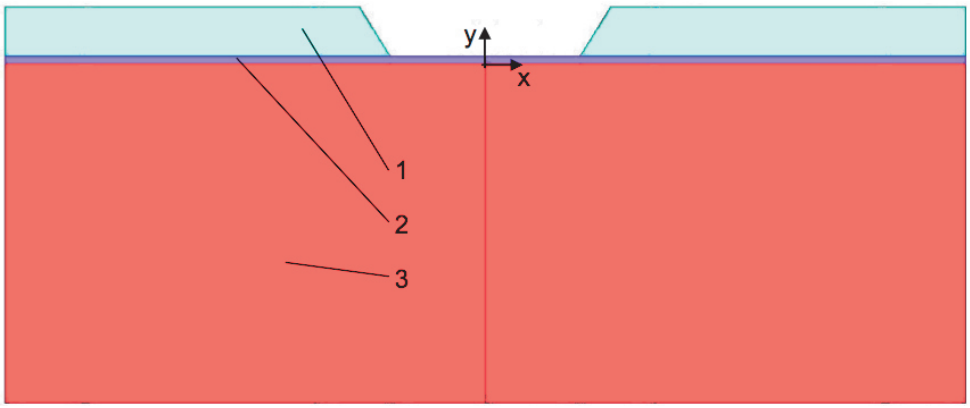

Fig. 2 Geometric model

Three materials (1, 2, 3) were used in the model. For this purpose model was divided into three zones, corresponding to them **Fig. 2**. Contact between the materials was ideal.

4.1 Mesh and geometry

Developed FE-model is presented in **Fig. 3**. Model is symmetrical about the *y* - axis.

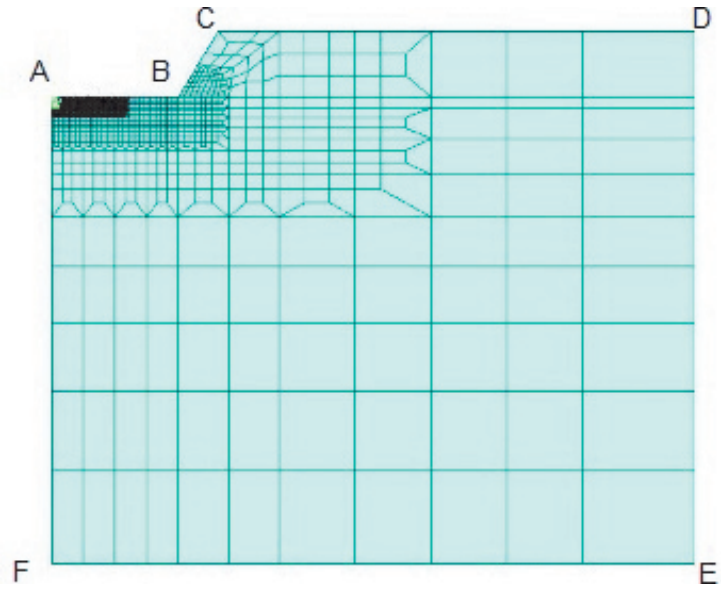

Fig. 3 A view of finite element mesh of friction stir welding plate

In the present thermal analysis, the workpiece is meshed using a simplex element called PLANE 55. A total of 3882 elements and 4003 nodes were generated in the model. The meshing strategy is about the smallest elements are located in the zone where biggest temperature gradient is expected.

4.2 Boundary conditions

The geometry and the boundary conditions of the developed model of FSW are shown in **Fig. 4**.

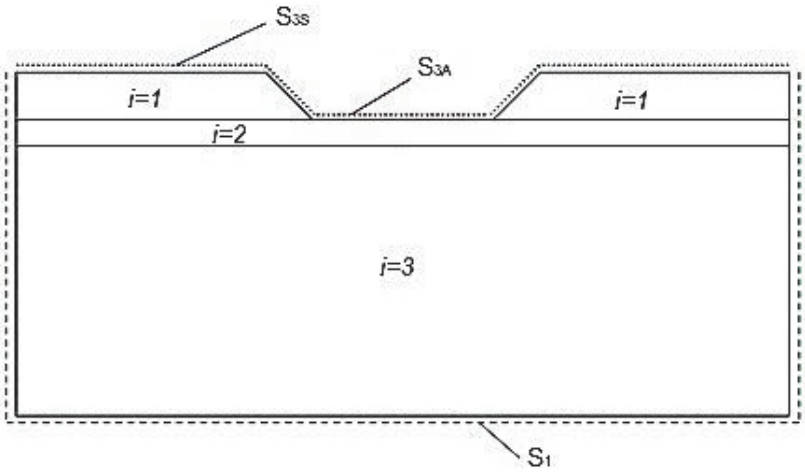

Fig. 4 Boundary conditions of the developed model

Material number is marked with *i*. The place where the temperature doesn't change during welding (first-order boundary) is marked with long dot-and-dash line. Position of the boundary or the distance from the heat source is defined by using analytical calculation of a fast-moving point heat source at the semi-infinite body [2]. The place where the third-order boundaries are situated is marked with short dot-and-dash line.

4.3 Assumptions und simplifications

Main simplification is the transition from 3D to 2D model. This simplification is made possible by the fact that heat source is a fast moving source along the *z* - axis perpendicular to the plane of the section. Heat transfer from the workpieces to the tool (model of plate, table and clamps) is negligible. Contact between the materials is ideal. Heat source is asymmetric. Metal is not melted during welding and geometry does not change. The slope of the tool in the direction of welding is not taken into account.

5. RESULTS AND DISCUSSION

Numerical maximum temperature distribution of the plate during FSW is shown in **Fig. 5**.

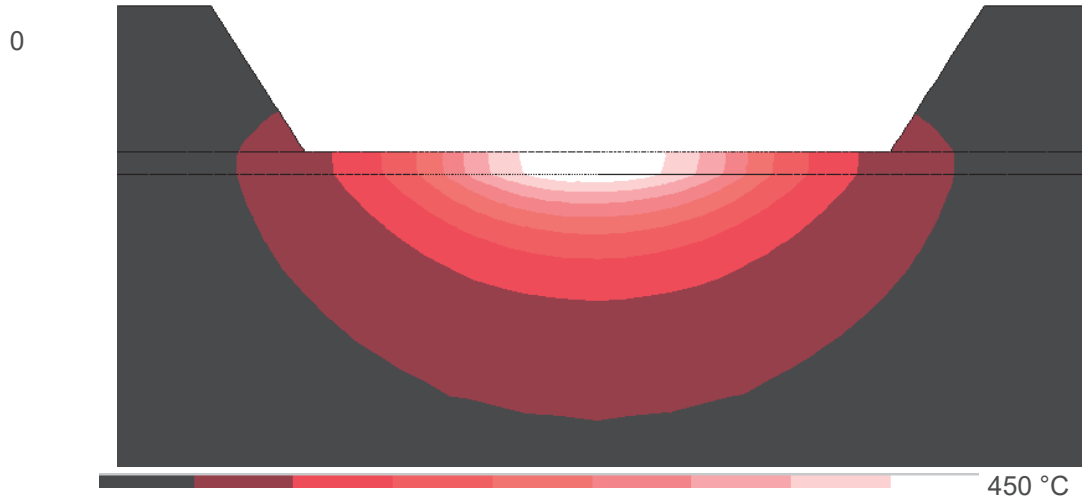

Fig. 5 Maximum temperature distribution

The comparison of numerical value and measured temperature distribution on the surface of the welded plates is shown in **Fig. 6** (*y* = 2).

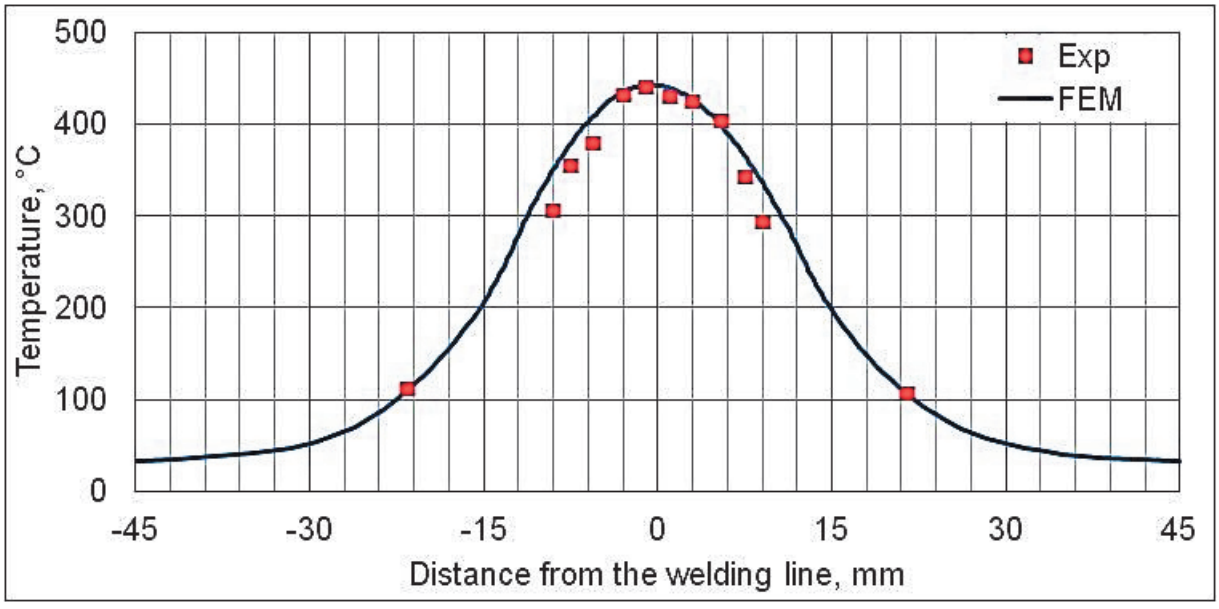

Fig. 6 Comparison of numerical value and measured temperature distribution

The experimental results are marked with dots and the numerical results are marked with line. The comparisons show that numerical results of temperature match with the experimental data very well.

CONCLUSION

All isotherms shown in **Fig. 5** pass through the backing plate and the workpiece. Heat flow during the FSW is directed to the backing plate. This means that the backing plate exerts great influence on the temperature distribution during FSW and cooling, i.e. backing plate material and the contact between the backing plate and workpiece. Clamps don't play a big role in the temperature distribution, because only one isotherm (50 °C) passes through them.

Heat source that used in the model is asymmetric consequently the temperature field must be asymmetric too. The difference between the temperatures on the advancing side and retreating side is visible in **Fig. 6**.

ACKNOWLEDGEMENTS

Financial support from the Ministry of Education and Science of the Russian Federation (Project 14.z50.31.0018) is gratefully acknowledged.

REFERENCES

[1] KAMMER, C. *Aluminium Taschenbuch 1 Grundlagen und Werkstoffe.* 16 Auflage, 2009, 764 p.

[2] РЫКАЛИН, К. Н. *Расчет тепловых процессов при сварке*, Moscow, Машгиз, 1951, 296 p.

[3] SCHMIDT, H. An analytical model for the heat generation in friction stir welding. *Modeling and Simulation in Materials Science and Engineering,* 2004, Vol. *12*, pp. 143-157.

[4] GEBHARD, P. *Dynamisches Verhalten von Werkzeugmaschinen bei Anwendung für das Rührreibschweißen.* Diss. Techn. Universität München, 2011.